AUTOMATIC BREAST CONTOUR DETECTION IN DIGITAL PHOTOGRAPHS

Jaime S. Cardoso, Luis F. Teixeira

INESC Porto, Faculdade de Engenharia, Universidade do Porto, Portugal

Maria J. Cardoso

Faculdade de Medicina, Universidade do Porto, Portugal

Keywords: Computer-aided medical system, breast cancer conservative treatment, breast contour, shortest path problem.

Abstract: Breast cancer conservative treatment (BCCT), due to its proven oncological safety, is considered, when feasible, the gold standard of breast cancer treatment. However, aesthetic results are heterogeneous and difficult to evaluate in a standardized way, due to the lack of reproducibility of the subjective methods usually applied. The objective assessment methods, considered in the past as being less capable of evaluating all aspects of BCCT, are nowadays being preferred to overcome the drawbacks of the subjective evaluation. A recent computer-aided medical system was developed to objectively and automatically evaluate the aesthetic result of BCCT. In this system, the detection of the breast contour on the digital photograph of the patient is a necessary step to extract the features subsequently used in the evaluation process. In this paper an algorithm based on the shortest path on a graph is proposed to detect automatically the breast contour. The proposed method extends an existing semi-automatic algorithm for the same purpose. A comprehensive comparison with manually-drawn contours reveals the strength of the proposed method.

1 INTRODUCTION

Breast cancer conservative treatment (BCCT) has been increasingly used over the last twenty years due to identical survival results when compared to mastectomy, and a better cosmetic outcome. Although considerable research has been put into the oncological aspects of BCCT, diverse aesthetic results are common due to the difficult standardization of this type of treatment, stressing the importance of the aesthetic evaluation in institutions dedicated to breast cancer treatment so as to improve working practices.

The first and more generalized methods used for aesthetic evaluation of BCCT were the subjective appreciation of the patient, directly or through photographs, by one ore more observers (Harris et al., 1979). The categorization of the aesthetic result, subjectively estimated and combined by observers through this visual inspection relies on the complex interplay of multiple factors. Considering the subjectivity of any human decision, the obtained results are questionable and frequently the reproducibility values obtained among observers are only modest. In fact,

this lack of reproducibility has been shown by others (Christie et al., 1996), which creates uncertainty when comparing results between studies. It has also been demonstrated that observers from different professional backgrounds evaluate cases differently, attaining even lower agreement results (Cardoso et al., 2005).

Objective methods of evaluation have emerged as a way to overcome these drawbacks of the subjective evaluation. Initially they consisted only in the comparison between the two breasts of simple measurements marked directly in patients or in photographs (Limbergen et al., 1989; Christie et al., 1996). The correlation of objective measurements with subjective overall evaluation has been reported by several authors (Christie et al., 1996). Trying to overcome the sense that objective asymmetry measurements were insufficient, other groups proposed the sum of the individual scores of subjective and objective individual indices (Al-Ghazal et al., 1999). More recently, a computer-aided medical system was developed to objectively and automatically perform the aesthetic evaluation of BCCT (Cardoso and Cardoso, 2007b). The

development of this system entailed the automatic extraction of several features from the photographs (Figure 1), capturing some of the factors considered to have impact on the overall cosmetic result: breast asymmetry, skin colour changes due to the radiotherapy treatment and surgical scar visibility. In a second phase, a support vector machine classifier was trained to predict the overall cosmetic result from the recorded features (Cardoso and Cardoso, 2007b).
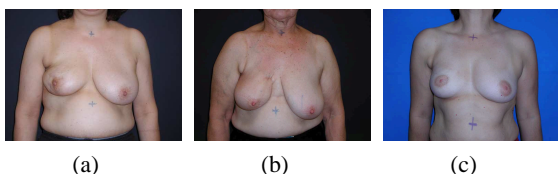

| (a) | (b) | (c) |

Figure 1: Typical photographs.

In order to extract the identified relevant features from the image, the detection of the breast contour is necessary. In (Cardoso and Cardoso, 2007a) the authors describe a *semi-automatic* method for the detection of the breast contour. The user has to *manually* identify the two endpoints of the breast contour. Subsequently, the algorithm automatically finds the contour in-between. The algorithm has been implemented in a computer-aided medical system: the software automatically finds the contours, extracts relevant features and outputs a predicted overall cosmetic assessment (*excellent*, *good*, *fair*, or *poor*).

Here, we improve on the work of (Cardoso and Cardoso, 2007a) in two different directions. First, we present an algorithm for the automatic detection of the endpoints of the breast contour, thus eliminating any user input from the process. Therefore a totally automatic breast contour detection is achieved. Next, we provide a thorough evaluation of the performance of the proposed method against manually-drawn breast contours. Standard metrics are employed to compare two contours.

Before presenting the proposed approach, and for completeness, we recover the framework for breast contour detection between two *known endpoints* of (Cardoso and Cardoso, 2007a). Then, in section 3 we detail how to automatically find the endpoints of a breast contour. Examples are provided and a performance analysis is conducted in section 4. Finally, in section 5, we conclude the paper and present possible directions of future work.

2 A SHORTEST PATH APPROACH TO CONTOUR DETECTION

When knowing the two endpoints of the breast contour, we are left with the problem of finding the path between both endpoints that goes through the breast contour. As the interior of the breast itself is essentially free of edges, the path we are looking for is the shortest path between the two endpoints, **if** paths (almost) entirely through edge pixels are favoured. More formally, let s and t be two pixels of the image and $\mathcal{P}_{s,t}$ a path over the image connecting them. We are interested in finding the path $\mathcal{P}$ that optimizes some predefined distance $d(s,t)$. This criterion should embed the need to favour edge pixels.

In the work to be detailed, the image grid is considered as a graph with pixels as nodes and edges connecting neighbouring pixels. Therefore, some graph concepts are in order.

2.1 Definitions and Notation

A *graph* $G = (V, A)$ is composed of two sets V and A. V is the set of nodes, and A the set of arcs (p, q), $p, q \in V$. The graph is *weighted* if a weight $w(p, q)$ is associated to each arc, and it is called a *digraph* if the arcs are directed, i.e., $(p, q) \neq (q, p)$. A path from p_1 to p_n is a list of unique nodes $p_1, p_2, \ldots, p_n$, $(p_i, p_{i+1}) \in A$. The *path cost* is the sum of each arc weight in the path.

In graph theory, the shortest-path problem seeks the shortest path connecting two nodes; efficient algorithms are available to solve this problem, such as the well-known Dijkstra algorithm (Dijkstra, 1959).

2.2 Proposed Algorithm

If the weight assigned to an edge captures the intensity of the contour of the adjacent pixels, finding the best contour translates into computing the minimum accumulated weight along all possible curves connecting s and t:

$$d(s,t) = \min_{\mathcal{P}_{s,t}} \sum w(p,q). \qquad (1)$$

Note that, if we ignore the weight component, we are simply computing the regular Euclidian distance between s and t along the path $\mathcal{P}_{s,t}$ (which will be a straight line for the shortest path).

Therefore, to detect the breast contour in (Cardoso and Cardoso, 2007a) it is proposed a two step approach:

1. Apply an edge detector to the original image (other operations, replacing the edge detector, will

be proposed latter in this work). The resulting binary image enhances the points of interest.

2. Detect the breast contour on the edge image, by finding the shortest path between the two endpoints.

We now detail this second step.

Starting by modelling the edge image as a graph, correspond a node to each pixel. Connect two nodes with an arc on the graph iff the corresponding pixels are neighbours (8-connected neighbourhoods) on the image. The weight of each arc is a function of pixels values and pixels relative positions — see Figure 2:
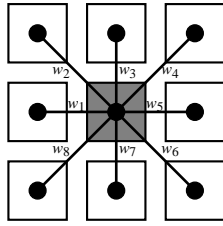

Figure 2: Arc weight between two pixels.

$$w_i = \begin{cases} f(p, q_i) \text{ if } q_i \in \text{4-connected neighbourhood of } p \\ h(p, q_i) \text{ if } q_i \notin \text{4-connected neighbourhood of } p \end{cases}$$

In this work we set $h(.,.) = \sqrt{(2)}f(.,.)$.

Now, to favour paths through edge pixels, one can set

$$f(p,q) = \begin{cases} c_1 \text{ if both p and q are edge pixels} \\ c_2 \text{ otherwise} \end{cases},$$

with $c_2 > c_1$. In this work c_1 and c_2 were experimentally determined as 2 and 32, respectively. Note that c_1 must be set greater than zero, to also favour the smallest path, when more than one exists through edge pixels only. Finally, the solution to the shortest path problem will yield the intended breast contour.

2.3 Algorithm Generalization

The proposed paradigm can be conveniently generalized. The application of an edge detector in the first step can miss to detect segments of the breast contour. This is especially true for women with small breasts (leading to weak contours) or when the breast is severely deformed with the excision of a large sample of tissue. A natural improvement is to replace the binary image outputted by the edge detector with a richer gradient image. Now, the shortest path algorithm should try to follow pixels with high gradient values. Thus, the $f(.,.)$ and $h(.,.)$ functions

have to be properly generalized. A simple strategy is to set $f(p,q) = \hat{f}(255 - \min(grad(p), grad(q)))$, where $\hat{f}(.)$ is a monotonically increasing function. Note that this more general setting has the binary case as a particular instantiation. To summarize, the proposed general framework to find the contour between two endpoints encompasses:

- A gradient computation of the original image. In a broader view, this can be replaced by any feature extraction process that emphasizes the pixels we are seeking for.

- Consider the gradient image as a weighted graph with pixels as nodes and edges connecting neighbouring pixels. Assign to an edge the weight $w_i = f(p,q)$ or $w_i = h(p,q)$, as described before.

The gradient model adopted in the experiments reported latter is based on the Sobel operator. The Sobel operator is applied on the x and y directions; from the computed values, S_x and S_y, the magnitude of the gradient is estimated as $z = \sqrt{S_x^2 + S_y^2}$. Costs were assigned based on an exponential law:

$$\hat{f}(z) = \alpha \exp(\beta z) + \delta, \quad \alpha, \beta, \delta \in \Re$$

The parameters α, β, δ were chosen to yield $\hat{f}(0) = 2$ and $\hat{f}(255) = 32$, leading to the same range of costs as the binary model. The third degree of freedom was experimentally tuned. The adopted transformation was (see also Figure 3) $\hat{f}(z) = 0.15 \exp(0.0208z) + 1.85$.
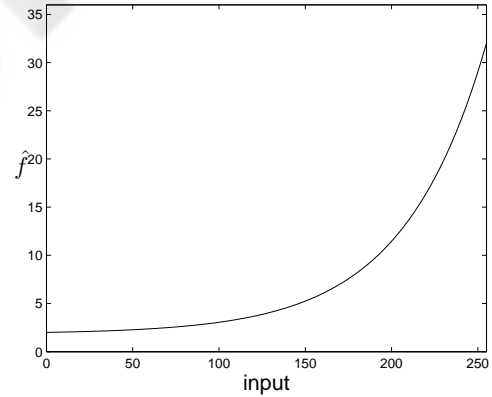

Figure 3: Transformation $\hat{f}(.)$.

3 AUTOMATIC DETECTION OF ENDPOINTS

The challenge now is to automatically extract the endpoints. In order to address this key problem we will

assume, very reasonably, that the photo contains only the torso of the patient.

The position of the *external* endpoint of the breast contour can be assumed at the point of the body where the arm contour intersects the trunk contour. However, because patients are in the arms-down position, the arm's contour is almost indistinguishable from the trunk's contour. Therefore, we define the external endpoint of the breast contour as the highest point of the trunk contour.

The approach just delineated requires first the detection of the trunk contour. That may be searched among the strongest lines of gradient with approximate vertical direction.

In order to get a first intuition of the general result, it is instructive to explore a basic example. Consider in Figure 4(a) the gradient intensity, with black pixels representing high intensity values.

(a) A single vertical line of nonzero gradient.

(b) The shortest path between some points on the bottom and the top margin.
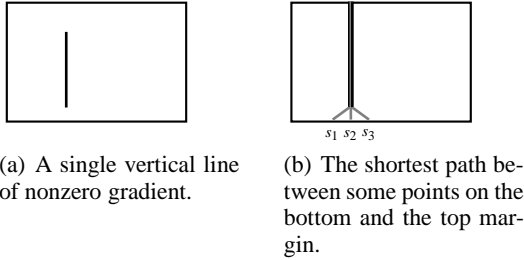
Figure 4: A first exemplificative example.

In Figure 4(b) the shortest paths between starting points s_i on the bottom row and the *whole* top row are traced. The distance between a *fixed* point on the bottom row and the whole top row can be generally formulated as the distance between a point s and a region Ω. The distance from a pixel s and a region Ω is given by

$$d(s,\Omega) = \min_{t \in \Omega} d(s,t), \qquad (2)$$

where $d(s,t)$ was defined previously. All the traced paths got attracted by the vertical line.

Phase 1: we propose to apply this procedure to the bottom half of our photographs:

1. Compute the gradient of the image (see Figure 5(a)).

2. Compute the shortest path between each point in the bottom row and the *whole* middle row of the gradient image (see Figure 5(b)).

3. Compute the shortest path between each point in the middle row and the *whole* bottom row of the gradient image (see Figure 5(c)).

4. Discard all paths except for those common to steps 2 and 3 (see Figure 5(d)).

5. Discard paths with a cost superior to half of the maximum possible cost (see Figure 5(e)). Finally, the trunk contour is defined as the two contours closest to the middle of the photograph.

(a) Gradient.

(b) Shortest paths from a pixel s in the bottom line and the whole middle row Ω_1, superimposed on the original image.

(c) Shortest paths from a pixel s in the middle row and the whole bottom row Ω_2, superimposed on the original image.

(d) Strong paths between the middle and bottom rows.

(e) Selected paths, superimposed on the original image.

(f) Strong paths between the top and bottom rows.

(g) The external endpoint of the breast contour is the highest point of the shortest path.

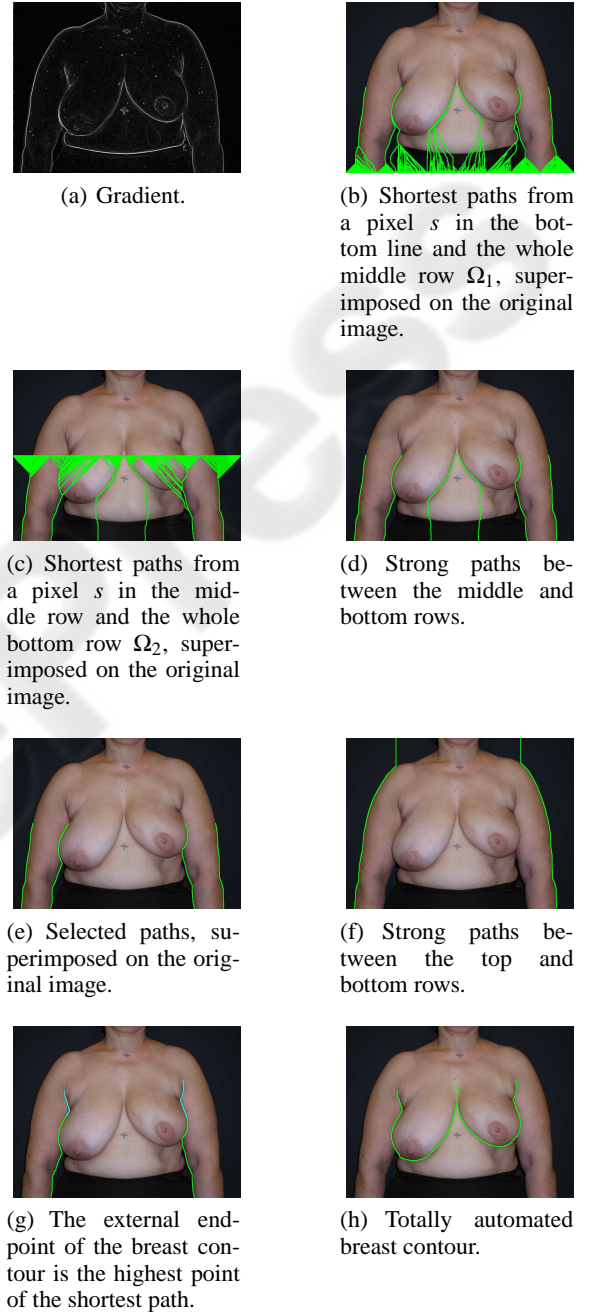(h) Totally automated breast contour.

Figure 5: Results for a real photograph.

It is appropriate to introduce now the concept of *strong path*.

Definition. A path $\mathcal{P}_{s,t}$ is a strong path between regions Ω_1 and Ω_2 if $\mathcal{P}_{s,t}$ is the shortest path between $s \in \Omega_1$ and the whole region Ω_2, and $\mathcal{P}_{s,t}$ is the shortest path between $t \in \Omega_2$ and the whole region Ω_1.

With this definition, steps 2, 3 and 4 are just the computation of the strong paths between the middle and bottom rows.

At the end of this phase we have already the position of the two trunk contours, but we have stopped the process at the middle of the image. Perhaps it is important to stress that if the process was conducted between the bottom and top rows, the trunk contours would be lost, as the only strong paths between the top and bottom rows would be the external silhouette of the patient (see Figure 5(f)) .

Phase 2: to determine the top of the trunk contour, we need to continue the path produced in phase 1 until a certain condition is met. Towards that end, we propose to find the shortest path between the ending point of the strong contour found in phase 1 and row $R_i, R_i = middle\_row, \cdots, top\_row$. We select the highest row for which the shortest path does not contain a long sequence (LENGTHTHRESHOLD) of consecutive pixels with low gradient (GRADIENTTHRESHOLD). Figure 5(g) illustrates the results obtained for the exemplificative photograph (LENGTHTHRESHOLD and GRADIENTTHRESHOLD were set to 12 and 48, respectively).

Before applying the algorithm presented in Section 2 to compute the breast contour we need also the internal endpoint of the breast contour. This was estimated simply as the middle point between the two external endpoints. Finally, the computation of the breast contour yields the result presented in Figure 5(h).

4 RESULTS

The methodology proposed in this paper was assessed on a set of photographs from 120 patients. The photographs were collected in three different institutions in Portugal. All patients were treated with conservative breast surgery, with or without auxiliary surgery, and whole breast radiotherapy, with treatment completed at least one year before the onset of the study. Breast images were acquired employing a 4M pixel digital camera. A mark was made on the skin at the suprasternal notch and at the midline 25 cm below the first mark (see Figure 1). These two marks create a correspondence between pixels measured on the digital photograph and the length in centimetres on the patient.

In order to investigate the possibility of defining an automated method of detecting the breast contour, a set of patients with known breast contour was required. Since, ideally, the automated method should correlate coherently with human assessment, eight different observers were asked to manually draw the contours. A software tool was developed specifically to assist on this job. The user defines the contour by positioning seventeen control points of cubic splines, see Figure 6.

Figure 6: Software for manual breast contour definition.

Before applying the proposed algorithm, each image was downsized to a constant width of 768 pixels, while keeping the aspect ratio. This improves the computational performance of the implementation of the software, without degrading the quality of the final result.

Figure 7 shows the evolution of the error when estimating the external endpoints' position of the breast contour. The error in pixels was scaled to centimetres with the help of the marks made on the skin of the patient. Table 1 summarizes the results.
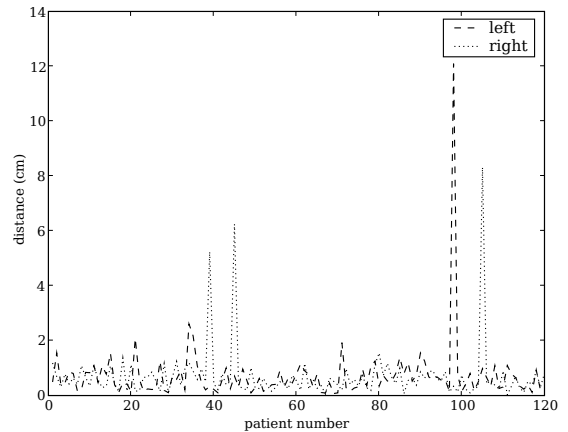

Figure 7: Evolution of error (cm) in the position of the external endpoints of the breast contour over 120 photographs.

Table 1: Mean, standard deviation and maximum value of errors in the position of the endpoints.

Error (cm)	mean	std dev	max
left endpoint	0.7	1.1	12.1
right endpoint	0.7	1.0	8.3
total	0.7	1.1	12.1

It can be observed that the proposed algorithm has a very interesting performance. The average error is quite low, less than 1 centimetre. Figure 8 shows some of the photographs for each the algorithm worked satisfactorily. It represents the result after the two phases of the algorithm. The highest point of the trunk contour provides the detected external endpoint of the breast contour. It is visible in patient #35 that the algorithm is robust against cluttered background. It is also visible in Figure 8 that, although the strong paths detected in phase 1 do not always correspond exactly to the trunk contour, the algorithm is still able to successfully detect the endpoints.
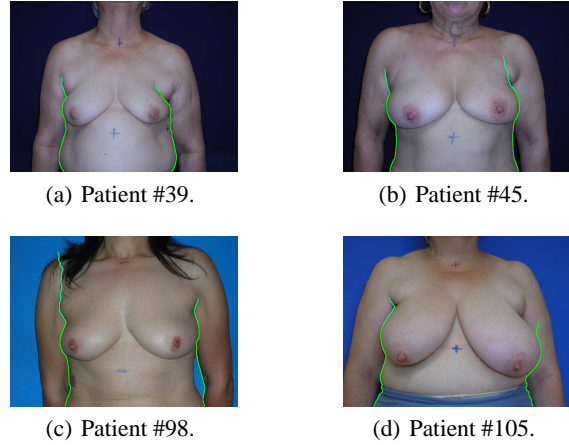

(a) Patient #05.   (b) Patient #22.   (c) Patient #35.

Figure 8: Selected successful results.

Nevertheless, four endpoints were clearly misplaced. These results, displayed in Figure 9, bring to light some of the limitations of the current state of the proposed approach. In patients #39, #45 and #105 the shortest path followed a 'wrong' contour, misplacing the endpoint. With patient #98 the long hair created a false 'path' till the top of the image.

After the automatic detection of the endpoints, the algorithm detailed in Section 2 to find the breast contour was applied to the photographs. Different scenarios can take place:

1. The endpoints were successfully located and the breast contour is correctly found. This desirable result is illustrated in Figure 10(a).

2. The endpoints were successfully located but the algorithm misses to follow adequately the breast contour (see Figure 10(b)).

3. The endpoints were poorly located but the algorithm rapidly finds and tracks the right breast contour (see Figure 10(c)).

4. The endpoints were poorly located and the breast contour is incorrectly tracked (this scenario did not occur in the experimental set of photographs).

(a) Patient #39.   (b) Patient #45.

(c) Patient #98.   (d) Patient #105.

Figure 9: All poor results.
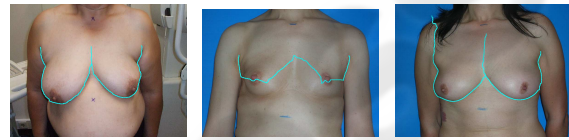
(a) Patient #35.   (b) Patient #114.   (c) Patient #98.

Figure 10: Breast contour results.

In a last set of experiments, the quality of the breast contour tracking algorithm was assessed. Instead of a simple subjective evaluation as provided in (Cardoso and Cardoso, 2007a), we conducted a complete objective evaluation, based on the hausdorff and the average distances to compare two contours. The hausdorff distance is defined as the "maximum distance of a set to the nearest point in the other set". Roughly speaking, it captures the maximum separation between the manual and the automatic contours. As observed in Figure 11 and Table 2 the experimental values obtained for the hausdorff distance correlate well with the error on the endpoints. This fact means that, most of the times, the major error on the automatic contour is located on the endpoint, with the shortest path algorithm recovering the true contour rapidly. A clear exception is patient #73, for which the error in the endpoints is negligible but the hausdorff distance between contours is very high. Here, the contour tracking algorithm missed to follow the contour, although it received proper endpoints.

The average distance between two contours captures better the perceived quality of the automatic breast contour. Here, the distance is averaged over the whole contour. Figure 12 and Table 3 summarize these results. As expected by visual inspection patient of #98 in Figure 10(c), although the error on the endpoint's location was high, the breast contour algo-
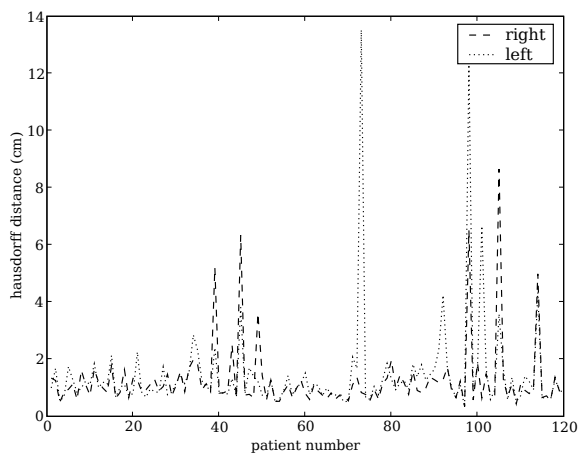
Figure 11: Evolution of hausdorff distance (cm) in the position of the breast contour over 120 photographs.

Figure 12: Evolution of the average distance (cm) in the position of the breast contour over 120 photographs.

Table 2: Mean, standard deviation and maximum value of hausdorff distance in the position of the breast contour.

Hausdorff dist. (cm)	mean	std dev	max
left endpoint	1.5	1.7	13.5
right endpoint	1.3	1.2	8.7
total	1.4	1.5	13.5

Table 3: Mean, standard deviation and maximum value of average distance in the position of the breast contour.

Average dist. (cm)	mean	std dev	max
left endpoint	0.2	0.6	5.2
right endpoint	0.1	0.3	2.4
total	0.2	0.4	5.2

rithm recovered rapidly, translated into a small average distance (but a high hausdorff distance).

The consequences of the diverse errors enumerated before to the computer-aided medical system are different and have to be further studied. For example, one of the features used for the objective aesthetic evaluation of the BCCT is the difference between the levels of inferior breast contour points. This measure is quite robust over strong errors on the endpoints' position, as long as the breast contour is correctly tracked. Other features, such as the difference in the area of the breast are much more sensible to the positioning of the endpoints. One line of future investigation is the selection of features robust to the common errors of the automatic detection of notable points (contour endpoints, breast contour, nipples, etc) but still capturing adequately the aesthetic result, leading to a good classification performance.
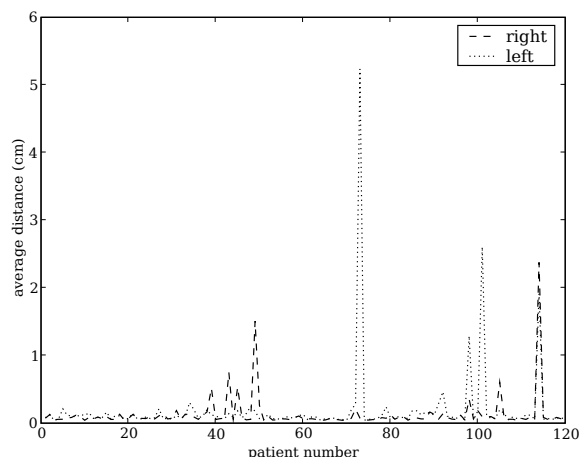
5 CONCLUSIONS

A method has been described for applying graph concepts to the task of automatically extracting the breast contour in digital photographs of the torso of a patient, after submitted to a breast cancer conservative treatment. In the proposed framework the problem of finding the endpoints of the breast contour is formulated as a problem of finding strong contours between two regions, a concept introduced here for the first time. The breast contour is found as the solution to the shortest problem on a graph, after conveniently modelling the image as a weighted graph. Preliminary results indicate an excellent performance in the task of finding the external endpoints of the contour and a good performance on detecting the breast contour. Future work will focus on improvements to the algorithm including generalizing the solution to other typical patient positions in these studies.

ACKNOWLEDGEMENTS

REFERENCES

Al-Ghazal, S. K., Blamey, R. W., Stewart, J., and Morgan, A. L. (1999). The cosmetic outcome in early breast cancer treated with breast conservation. *European journal of surgical oncology*, 25:566–570.

Cardoso, J. S. and Cardoso, M. J. (2007a). Breast contour detection for the aesthetic evaluation of breast cancer conservative treatment. In *International Conference on Computer Recognition Systems (CORES'07)*.

Cardoso, J. S. and Cardoso, M. J. (2007b). Towards an intelligent medical system for the aesthetic evaluation of breast cancer conservative treatment. *Artificial Intelligence in Medicine*, 40:115–126.

Cardoso, M. J., Santos, A. C., Cardoso, J. S., Barros, H., and Oliveira, M. C. (2005). Choosing observers for evaluation of aesthetic results in breast cancer conservative treatment. *International Journal of Radiation Oncology, Biology and Physics*, 61:879–881.

Christie, D. R. H., O'Brien, M.-Y., Christie, J. A., Kron, T., Ferguson, S. A., Hamilton, C. S., and Denham, J. W. (1996). A comparison of methods of cosmetic assessment in breast conservation treatment. *Breast*, 5:358–367.

Dijkstra, E. W. (1959). A note on two problems in connexion with graphs. *Numerische Mathematik*, 1:269–271.

Harris, J. R., Levene, M. B., Svensson, G., and Hellman, S. (1979). Analysis of cosmetic results following primary radiation therapy for stages i and ii carcinoma of the breast. *International Journal of Radiation Oncology Biology Physics*, 5:257–261.

Limbergen, E. V., Schueren, E. V., and Tongelen, K. . V. (1989). Cosmetic evaluation of breast conserving treatment for mammary cancer. 1. proposal of a quantitative scoring system. *Radiotherapy and oncology*, 16:159–167.